J Nanostruct 11(1): 81-94, Winter 2021

RESEARCH PAPER

Green Synthesis of CuO Nanostructures using *Syzygium guineense (Willd.)* DC Plant Leaf Extract and Their Applications

Tegene Desalegn[1], H C Ananda Murthy[1,*], C R Ravikumar[2], H P Nagaswarupa[3]

[1] *Department of Applied Chemistry, School of Applied Natural Science, Adama Science and Technology University, P O Box 1888, Adama, Ethiopia*

[2] *Research Centre, Department of Science, East West Institute of Technology, Bangalore, 560091, India*

[3] *Department of Chemistry, Davanagere University, Shivagangothri, Davanagere, 577001, India*

ARTICLE INFO

Article History:
Received 21 September 2020
Accepted 03 December 2020
Published 01 January 2021

Keywords:
Antibacterial activity
Green synthesis
Medicinal plants
Syzygium guineense (Willd.) DC
SyG-CuO NSs

ABSTRACT

The medicinal plant, Syzygium guineense (Willd.) DC (Waterberry) mediated green copper oxide nanostructures (SyG-CuO NSs) were successfully synthesized for the first time in Ethiopia. The antibacterial activity of CuO NSs capped by biomolecules of the plant leaf extract has been investigated. The UV-visible, UV-DRS, FT-IR, XRD, TGA-DTA, SEM, EDXA, TEM, HRTEM and SAED techniques were employed to characterize the NSs. The presence of two absorbance maxima, $\lambda_{max}1$ and $\lambda_{max}2$ at 423 nm and 451 nm, respectively confirms a mixture of copper oxide (E_g=1.93 eV). FTIR spectra confirmed the presence of biomolecules with SyG-CuO NSs. The XRD patterns of NSs confirmed the presence of CuO with high crystallinity. The purity of the NSs was confirmed by SEM-EDAX analysis. In addition, TEM-HRTEM-SAED analysis revealed the d-spacing value of 0.2854 nm which corresponds to CuO (111) lattice fringe. SyG-CuO NSs showed good antibacterial effect against both Gram-positive bacteria, S. aureus (12 mm), and Gram-negative bacteria, E. coli (12 mm), P. aeruginosa (10 mm), and E. aerogenes (12 mm). The bioactive compounds capped around the CuO NPs served the effective role in disrupting the cell wall of bacterial strains. The CV and EIS studies confirmed the better electrochemical properties for SyG-CuO with low charge transfer resistance value of 49 Ω. These CuO NSs exhibited multifunctional applications.

How to cite this article
Desalegn T., Murthy H.C.A, Ravikumar C.R., Nagaswarupa H.P. Green Synthesis of CuO Nanostructures using Syzygium guineense (Willd.) DC Plant Leaf Extract and Their Applications. J Nanostruct, 2021; 11(1): 81-94. DOI: 10.22052/JNS.2021.01.010

INTRODUCTION

Ethiopia has very rich biodiversity in the world with 6,500 species of higher plants. Most of the rural population of Ethiopia is dependent on traditional medicine who have little access to health services. In recent years numerous Ethiopian medicinal plants have been validated in a scientific empirical framework through phytochemical analysis and subsequent bioassays [1]. The medicinal plants species have been applied to treat many diseases.

* *Corresponding Author Email: anandkps350@gmail.com*

Syzygium guineense (Willd.) DC is a medium-sized or tall evergreen tree with the height of 15-30 m. The ripe fruits are consumed by humans, birds, and some wild animals. The bark varies in subspecies and is greyish-white or silver mottled and smooth in young trees, turning rough, flaky, creamy, light grey, dark brown or black in older trees. Fruit of this plant is used as a remedy for dysentery, while a decoction of the bark is used as an anti-diarrhoeic. In traditional medicine, liquid from the

This work is licensed under the Creative Commons Attribution 4.0 International License.
To view a copy of this license, visit http://creativecommons.org/licenses/by/4.0/.

pounded bark and roots, mixed with water, is used as a purgative. This plant has been identified for our present work to synthesise CuO NSs.

The research on the fabrication of plant mediated CuO NSs for biomedical, environmental and agricultural applications has gained significance in the recent years. The green CuO NSs have been used for photocatalytic, organic dye degradation, biomedical, pharmaceutical, cosmetic, energy and catalytic applications since many decades [2]. These CuO nanostructures such as nanoparticles, nanocrystals, nanorods, nanotubes, nanosheets exhibit versatile properties and hence found to be more useful when combined as coatings in textiles for antifungal and antimicrobial applications. The nanoparticles of copper and its oxides have shown great promise as antibacterial agent. A very few medicinal plants such as *Barleria prionitis* [3], *Dioscorea bulbifera* [4], *Caesalpinia bonducella* [5], *Hagenia abyssinica* [6][7] have been used to synthesize silver, gold, copper and their oxides in the recent past for antimicrobial applications. But no significant work has been done especially with the application of medicinal plant extracts as reducing and capping agents for the synthesis of CuO NSs in Ethiopia for biomedical and antibacterial applications. Thus we present the eco-friendly green synthesis of CuO NSs using medicinal plant *Syzygium guineense (SyG)* leaf extract at low temperature to investigate the influence of phytochemicals capped CuO NSs on bacteria with evaluation of electrochemical properties.

MATERIALS AND METHODS

Chemicals

The chemical Cu $(NO_3)_2{\cdot}3H_2O$, ethanol, Dimethyl sulfoxide DMSO used in the experiments were of analytical grade (purchased from Merck chemical Industrial company).

Collection and authentication of plant materials

Syzygium guineense (Willd.) DC plant leaves were collected from the Arsi zone, Ethiopia. The identity of the plant *Syzygium guineense* (Willd.) DC. (Code EB006) was authenticated by a plant taxonomist at the National Herbarium, Department of Biology, Addis Ababa University Herbarium, Addis Ababa, Ethiopia.

Preparation of plant leaf extract

The young leaves of *Syzygium guineense* were picked and washed repeatedly with tap water followed by distilled water and then shade dried for 15 days to remove moisture contents from the leaves. The procedure to prepare the extract is followed as per our reported work [8] and hence not discussed here.

Green synthesis of SyG- CuO *NSs*

A standard 0.2M aqueous Cu $(NO_3)_2{\cdot}3H_2O$ solution was prepared. The plant leaf extract (100 ml) was added to 400 ml of 0.2M Cu $(NO_3)_2{\cdot}3H_2O$ solution (1:4) dropwise with constant stirring [9] at about 45 °C. Then the solution was centrifuged for 20 min at 8000 rpm after completion of incubation at room temperature for 24 hrs. The obtained *SyG*-CuO NSs were washed by deionized water and ethanol to remove any impurities. Thereafter, the NSs were dried ground and stored for further analysis [10].

Characterization Techniques

The UV-visible absorbance and reflectance spectra of the samples were recorded in the range of 200–800 nm using Shimadzu's UV-2600, UV-visible spectrophotometer. The thermal stability of the CuO was conducted with TGA/DTA instrument (DTG 60H Shimadzu Co. South Korea). *Fourier* transform-infrared spectroscopy (FT-IR) Spectrum was recorded using 65 FT-IR PerkinElmer. X-ray diffraction (XRD-Shimadzu x-ray diffractometer (PXRD-7000) analytical technique was used to reveal the crystalline nature of CuO NSs [11]. Microscopic analysis has been conducted by scanning electron microscopy with energy-dispersive X-ray spectroscopy (SEM-EDX-EVO 18 model with low vacuum facility and ALTO 1000 Cryo attachment) and transmission electron microscope with high-resolution (JEOL JEM 2100 HRTEM) Gatan Digital Micrograph Software was used to evaluate d-spacing values of lattice fringes. Particle size was obtained by using imageJ application.

Method of antimicrobial evaluation

All the antibacterial tests were conducted at Oromia Public Health Research, Capacity Building & Quality Assurance Laboratory, Adama, Ethiopia. The *in-vitro* antibacterial activity of *SyG*-CuO NSs was evaluated using Agar disc-diffusion method against selected one Gram positive bacteria (*Staphylococcus aureus*) and three Gram negative pathogenic bacteria (*Escherichia*

CC BY

Table 1. The details of phytoconstituents screening of *Syzygium guineense* Plant leaf extract.

Sl. No.	Phytoconstituents	Test / Reagent	Result
1	Alkaloids	Wagner's reagent	+
2	Tannins	KOH	+
3	Flavonoids	Shinoda Test	-
4	Terpenoids	Salkowski Test	-
5	Anthraquinone glycosides	Borntrager's Test	+
6	Cardiac glycosides	Keller-Kiliani Test	+
7	Saponins	Frothing Test+	+
8	Phenols	$FeCl_3$	+

coli, *Pseudomonas aeruginosa and Enterobacter aerogenes*). A standardized inoculum of the bacteria was swabbed onto the surface of Mueller-Hinton Agar (MHA) plate. The actively growing bacterial cultures were inoculated/ spread onto the MHA plate (turbidity was adjusted with TSB to match 0.5 McFarland standard) The nanoparticles extract was prepared with four different concentrations in Dimethyl Sulfoxide. Four concentrations (6.25, 12.5, 25 and 50 µg/µl) of the synthesized nanoparticles were added to the respectively labeled wells.

The antibiotic discs of 6 mm diameter were applied to agar surface using forceps with gentle pressure and then impregnated with the dissolved extract. Chloramphenicol disc was used as a positive control while DMSO was taken as negative control. The plates were incubated at 35 ±2°C in an ambient air incubator for 18-24 hours. The antimicrobial activity was evaluated in terms of zone of inhibition, measured to the nearest millimeters (mm) using a ruler and recorded [12].

Electrochemical Test

Cyclic voltammetric tests were conducted by using CHI608E potentiostat. The potential range utilized during these studies is ranging between −0.6 V and 0.6 V. EIS studies were carried out in the frequency range of 1 Hz to 1 MHz at AC amplitude of 5 mV [13].

RESULTS AND DISCUSSION

Synthesis and Characterization of SyG-CuO NSs

The *SyG-CuO* NSs were synthesized by using copper nitrate as a precursor and *Syzygium guineense* plant leaf extract as a reducing and capping agent. The biomolecules present in the extract were alkaloids, phenolic compounds, tannins, saponins, anthraquinone glycosides and cardiac glycosides. The details of the phytochemical screening are as given in Table 1. The reactive hydrogen atom released during tautomeric transformation of polyphenols from enol form to keto form would reduce copper ions to copper nanoparticles. In addition, the enzymes of leaf extract also assist copper ions to form an enzyme substrate complex resulting into formation of protein capped copper NSs [14]. It is also understood that polyphenols bind copper ions and reduce them and cap them to form nanostructures. These polyphenolic ligands are believed to influence the morphology of formed particle as reported by the earlier researcher [15].

The as synthesised *SyG*-CuO NSs were characterized using UV-visible, UV-DRS, FT-IR, XRD, SEM, EDXA, TEM, HRTEM and SAED techniques. The UV-visible absorbance spectrum recorded for instantaneously synthesised *SyG*-CuO NSs exhibited λ_{max} of 423 as shown in Fig. 1a, just after 10 min of mixing plant extract with copper nitrate solution. This absorption band is basically due to surface plasmon resonance of *SyG*-CuO NSs. The absorbance spectrum recorded after 40 minutes of forming homogeneous mixture, exhibited 2 maxima, one λ_{max} at 423 nm and the other at λ_{max} of 451 nm (Fig. 1b). The splitting of absorbance band into two, clearly confirm the formation of more than one type of nanoparticles.

The presence of two maxima is the clear indication of a mixture of copper and its oxides NSs. Initially Cu-NSs formed resulted in a single band with λ_{max} of 423 nm. But at later stage, Cu is found to react slowly and undergo surface oxidation to CuO. This is responsible for the presence of 2 maxima in the spectrum after 40 minutes of beginning of synthesis process of NSs. A similar result was observed during the analysis of synthesized CuO NSs using the *Zingiber and Allium sp.* [16] and *Psidium guajava* leaves extract [17]. The surface plasmon absorbance presents a set of different λ_{max} values for NSs synthesised using different plant extracts which is possibly influenced by morphological features of the NSs.

Similarly, the UV-visible diffused reflectance

CC BY

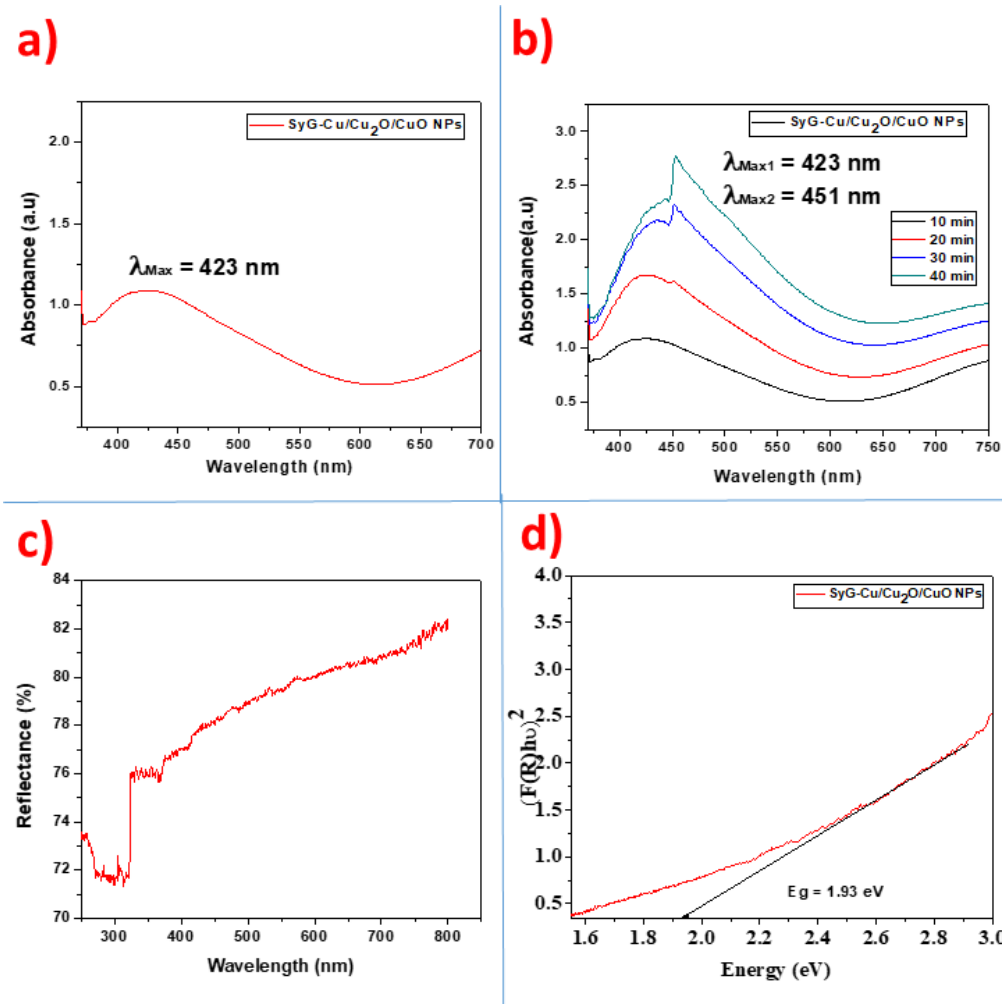

Fig. 1. (a) and (b) UV-visible absorbance spectrum of *SyG*-CuO NSs at different time intervals (c) UV-visible diffused reflectance spectrum of *SyG*-CuO NSs. (c) Tauc plot of *SyG*-CuO NSs showing E_g Value.

spectrum was recorded (Fig. 1c). The band gap energy of *SyG*-CuO NSs obtained by Tauc plot using the data obtained in reflectance spectra utilizing Kubelka-Munk function is as shown in Fig. 1d. The band gap energy, E_g of *SyG*-CuO NSs was found to be 1.93 eV.

The XRD analysis was executed to explore the in-depth details of crystal structure of VeA-CuO NPs. The XRD spectrum of SyG-CuO NSs (Fig. 2) demonstrates a total of 11 prominent peaks [7] .

The other peaks at 2θ values of 32.46°, 35.52°, 38.73°, 48.81°, 53.42°, 58.01°, 61.53°, 66.09° 67.98°, 72.48° and 75.13° correlates to 110, 002, 111, 20-2. 020, 202, 11-3, 31-1, 113 and 400 planes of CuO (fcc) (ICSD card No. 00-048-1548, Tenorite-C2/c)) [18]. This confirms the formation of crystalline CuO from the plant extract via green synthetic route [19]. The main draw back in the green synthesis of copper nanoparticles is their rapid oxidation in air to yield Cu_2O and CuO [20]. It is believed that Cu and Cu_2O formed at the initial stages of biosynthesis would have oxidized on exposure to air for a longer period of time. However, trace amounts of Cu and Cu_2O were detected during selective area electron diffraction (SAED) experimentation which has been clearly discussed under SAED analysis section.

The FTIR spectra of *SyG* plant extract and *SyG*-CuO NSs are shown in Fig. 3. FTIR spectra confirmed the presence of biomolecules in the extract and NSs. The broad peaks appeared in the region between 3391 and 2926 cm^{-1} corresponds to –OH stretching vibration and sp^3 C-H stretching vibrations, respectively. The peak at 1623 cm^{-1}

CC BY

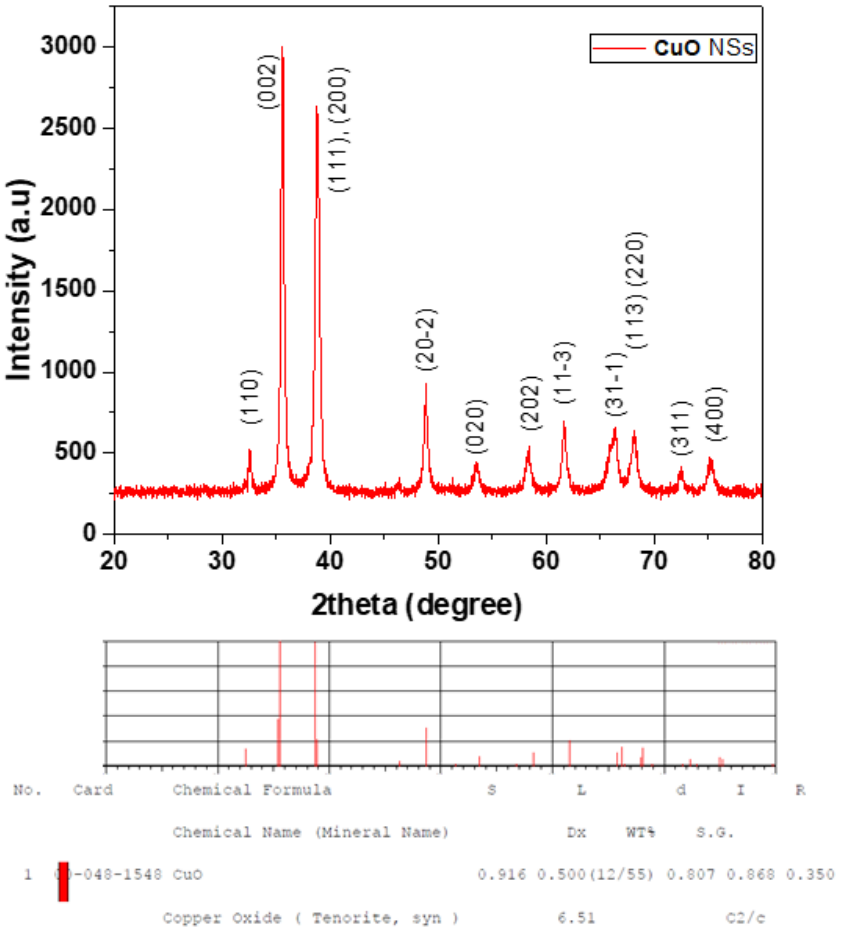

Fig. 2. The XRD pattern of *SyG*-CuO NSs.

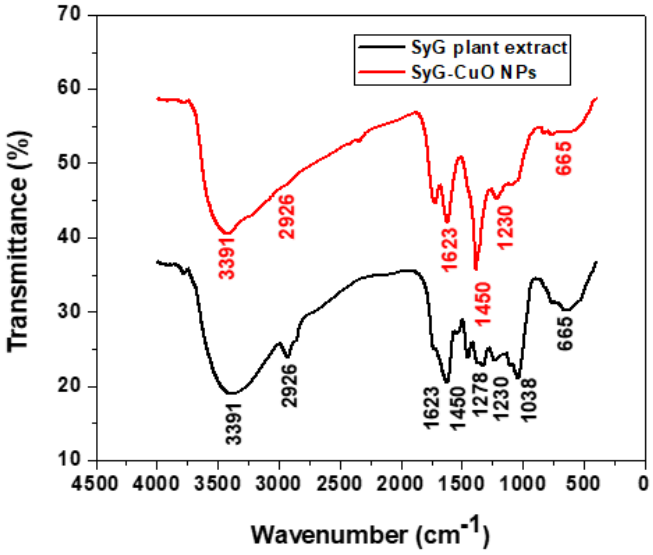

Fig. 3. The FTIR spectra of *SyG* plant extract and *SyG*-CuO NSs

CC BY

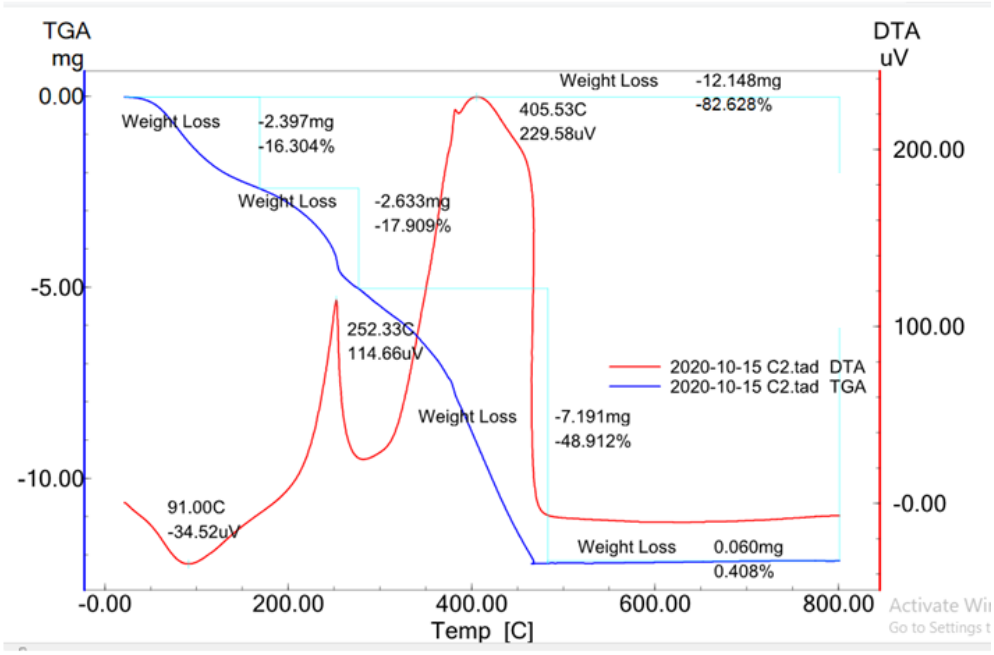

Fig. 4. TG /DTA curves of *SyG*-CuO NSs

corresponds to C=O stretching of carbonyl groups. The sharp peak around 1450 cm^{-1} shows the presence of −COO group of carboxylic acid. It is also believed that the amine and carboxylate group present in the SyG plant leaf extract responsible for the binding of proteins with the surface of CuO and thereby leading to the stabilization of the biosynthesized nanoparticles. The intense peaks shown at 3391 cm^{-1}, 1278 cm^{-1} and 1230 cm^{-1} corresponds to phenolic –OH stretching and bending vibrations.

The peaks at 1450 cm^{-1}, 1623 cm^{-1} and 2926 cm^{-1} corresponds to −COO group of carboxylic acid, C=O stretching of ketonic groups and alkane C–H stretching mode respectively. A less intense peak at around 750 cm^{-1} confirms the presence of glycosidic linkage. The presence of prominent peaks at 3391 cm^{-1}, 2926 cm^{-1}, 1623 cm^{-1}, 1450 cm^{-1} and 665 cm^{-1} in the FTIR spectra of both plant extract and NSs, clearly indicate the presence of bioactive molecules around the NSs. These phytochemical have played a significant role in the nucleation and growth of *SyG*-CuO NSs and hence found to be at the surface of nanostructures [21].

The bending vibrations of Cu–O–H bonds resulted in a small peak at 750 cm^{-1} which can be attributed to the presence of the Cu–O bond. The last peak at 665 cm^{-1} corresponds to bending modes of vibrations of C–H bond. FTIR analysis results confirmed the presence of various phytochemicals of the leaf extract such as phenolics, tannins, glycosides and proteins which played the roles of reducing agent and stabilizing agent during the synthesis of *SyG*-CuO NSs.

Fig. 4 presents the TGA-DTA curves for the thermal transformation of *SyG*-CuO NPs on heating from 0 to 800 °C under oxygen. The TGA curve revealed the three-step decomposition of CuO NSs, with the weight loss occurring in the temperature ranges of 30−160 °C, 160−270 °C and 270−480 °C. About 16 % weight loss was observed in the first temperature region due to usual water evaporation from the NSs. Similarly, 2nd and 3rd weigh losses were recorded to an extent of 17 % and 48 % corresponding to the decomposition of capped biomolecules on the NSs. The presence of different types of capped biomolecules are believed to be responsible for two stages of decomposition during TGA studies.

Figure 4 also shows a small endothermic DTA peak at the region of 91 °C, which corresponds to the first mass loss in the TGA curve. The second weight loss occurring around 160−270 °C in TGA is associated with a prominent DTA exothermic peak at 252 °C. The third major weight loss of 48 % at 405 °C (DTA exothermic peak) corresponds to complete

CC BY

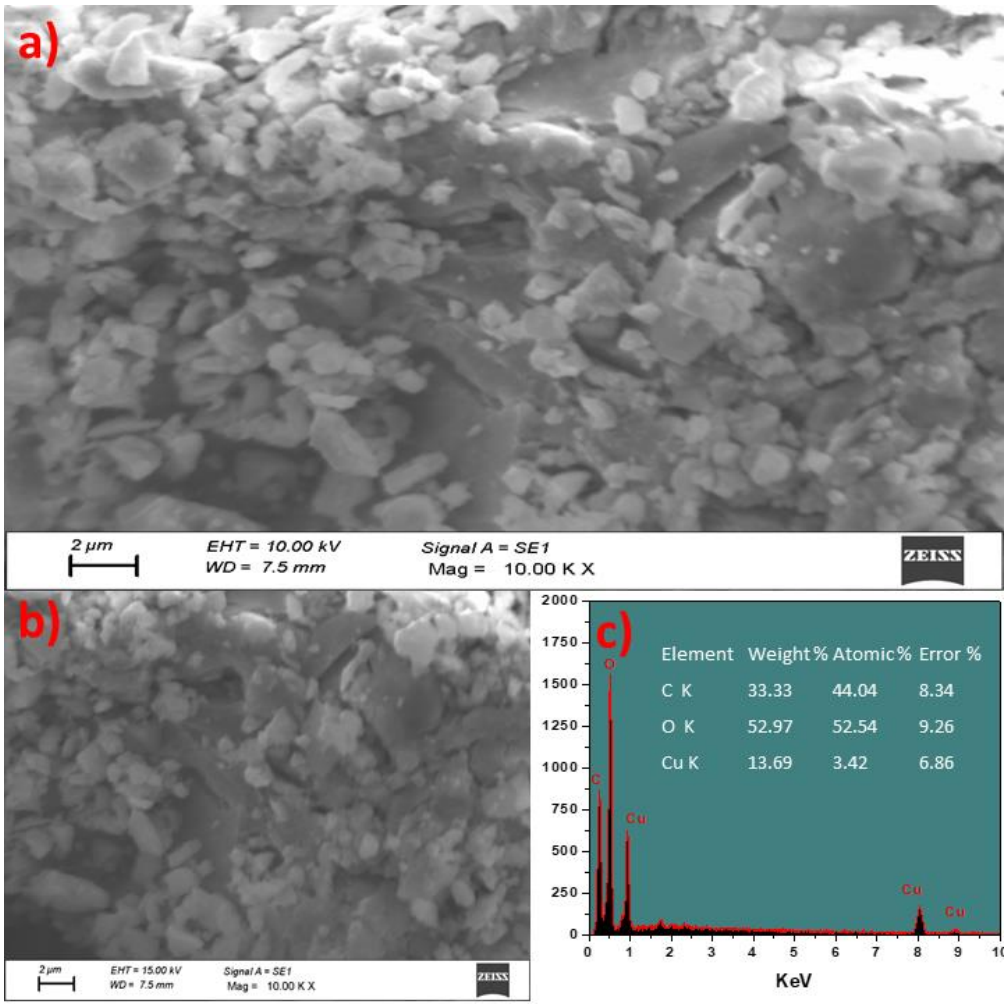

Fig. 5. (a), (b) and (c) SEM micrographs of *SyG*-CuO NSs (d) EDAX spectrum of *SyG*-CuO NSs.

decomposition of bioorganic phytoconstituents present around CuO NPs.

The morphological features of synthesized *SyG*-CuO NSs as depicted by SEM micrographs are shown in Fig. 5a and 5b. The SEM images also presented various types of nanoparticles in terms of their shape and size.

The average grain size of CuO NSs was found to be in the range between 5 and 50 nm [22]. The presence of mixed type of NSs is possibly due to the amount of capping agents around the particles [23]. EDAX analysis revealed the elemental composition of the *SyG*-CuO NSs as depicted in Fig. 5c. The peaks corresponding to elemental Cu, C and O were clearly identified demonstrating the purity of the synthesized NSs and this is consistent with the XRD studies. No additional impurity peaks were observed.

The presence of elements, C and O can be attributed to capped bioactive compounds. In addition, it is also apprehended that copper present at the surface had been converted into CuO. In addition, it is also expected that copper, on exposure to air, is oxidized to yield very small amounts of CuO and Cu_2O. The reduction of copper ions to Cu NSs is facilitated by the biomolecules of plant extract containing surface hydroxyl groups. In order to explore deep insights on the morphology, size and crystalline nature of the *SyG*-CuO NSs, TEM, HRTEM and SAED micrographs and patterns were utilized. The HRTEM images of as-synthesized *SyG*-CuO NSs (Fig. 6) shows that the synthesized NSs are nearly spherical but exhibited varieties of shapes. The presence of small particle

(cc) BY

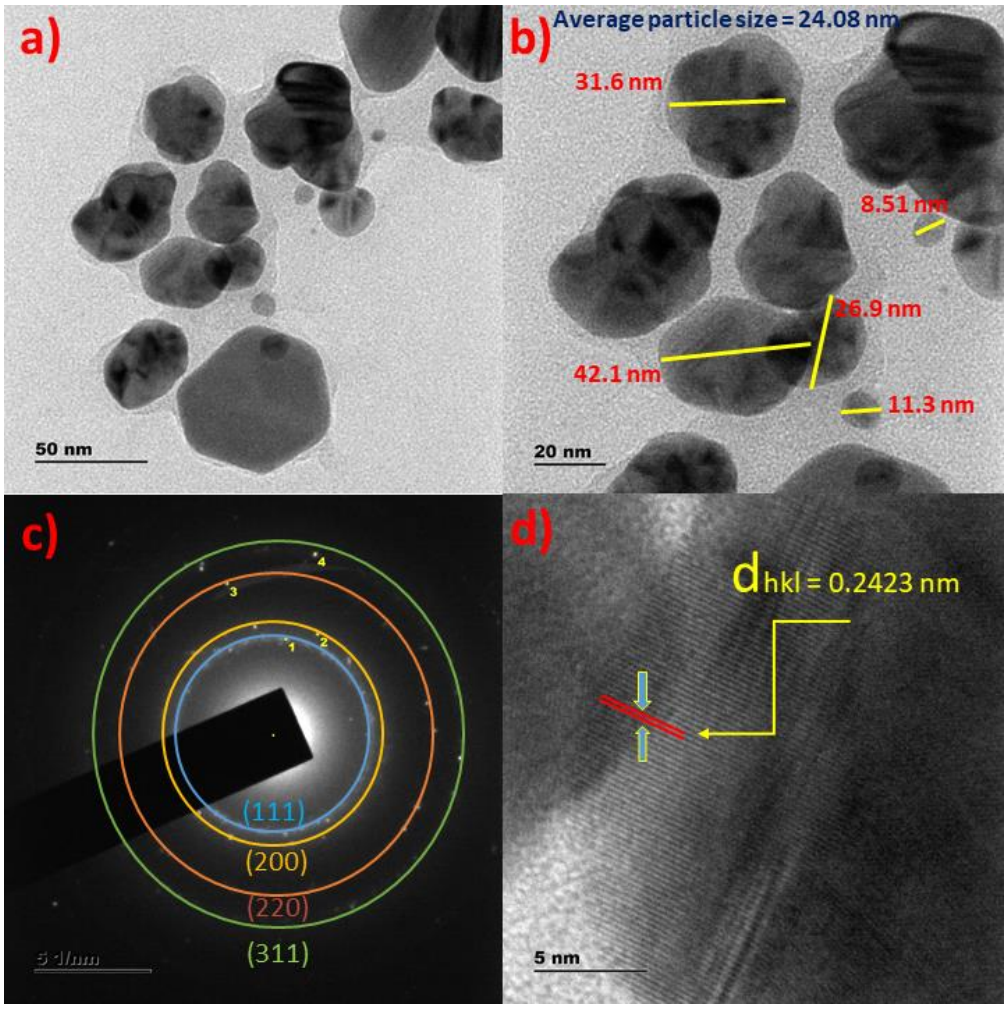

Fig. 6. TEM images of as-synthesized *SyG*-CuO NSs at (a) lower magnification (100 nm) and (b) higher magnification (50 nm) (c) SAED pattern with 1 to 4 spots and (d) HRTEM image showing lattice fringes of *SyG*-CuO NSs with d-spacing of 0.2423 nm.

with size 4.6 nm confirm efficiency of bioactive components of plant extract as capping and stabilizing agents. The nearly spherical particles with varying sizes from 8.1 nm to 42.1 nm with an average particle size of 24.08 nm as determined by imageJ application are as shown in Fig. 6a and 6b.

The six spots corresponding to specific crystal planes were observed on SAED pattern of *SyG*-CuO NSs (Fig. 6c). One of such planes is presented with d-spacing of 0.2423 nm as shown in Fig. 5d.

The Fig. 7a, 7b and 7c presents the HRTEM micrographs with *SyG*-CuO NSs with magnified lattice fringes, IFFT patterns and profile of IFFT with d-spacing value for a specified plane (Fig. 6d) respectively. The d_{hkl} value of 0.2423 nm for a specific set of crystal planes at the surface of Cu NSs was deduced by using Gatan Digital Micrograph Software application.

The d-spacing values for all the spots depicted in the SAED pattern of *SyG*-CuO NSs (Fig. 6c) are presented in Table 2. Each spot on the SAED pattern corresponds to specific set of lattice planes.

The presence of 4 major peaks corresponding to (111), (200), (220) and (311) planes of fcc structure of pure CuO in the XRD pattern of NSs was presented earlier as Fig. 2. The d-spacing values of the derived diffraction planes from spot 1 to spot 4 corresponds to d_{-111}CuO = 0.2854 nm, $d_{111}Cu_2O$ = 0.2432 nm, d_{200}Cu = 0.2271 nm and d_{111}Cu = 0.2040 nm respectively. The absence of Cu and Cu_2O peaks in the XRD pattern can be possibly due to their presence in very small quantities.

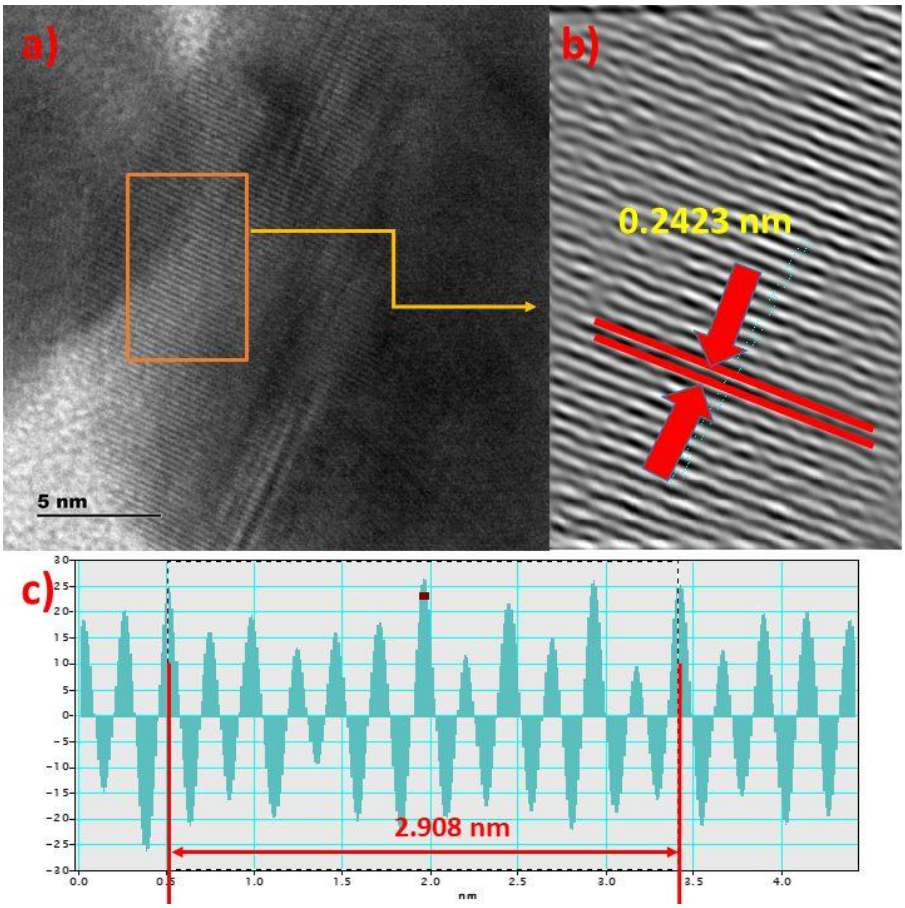

Fig. 7. HRTEM morphology of *SyG*-CuO NSs (a) Magnified lattice fringes (b) IFFT patterns (c) Profile of IFFT with d-spacing distance.

Table 2. The d-spacing values for *SyG*-CuO NSs from SAED pattern.

Spot No.	d- spacing (nm)	Rec. Pos. (1/nm)	Degrees to Spot 1	Amplitude
1	0.2854	3.504	0.00	284.20
2	0.2432	4.112	11.68	1093.93
3	0.2271	4.404	9.20	612.11
4	0.2040	4.903	30.11	178.68

This SAED-HRTEM analysis is in good agreement with the previously arrived XRD results for the *SyG*-CuO NSs. The d-spacing value of lattice fringes at the surface of the *SyG*-CuO NSs was found to be 0.2395 nm, which is similar to the d_{hkl} value of 0.24 nm for (111) plane of fcc structured Cu_2O obtained in the previous reported work [24]. This confirms that the copper atoms at the surface of NSs reacted with air to form their respective oxides, Cu_2O and CuO.

Antimicrobial activity

The *SyG*-CuO NSs exhibited broad range of antibacterial activities against all tested pathogens; *S. aureus, E. coli, P. aeruginosa,* and *E. aerogenes.* The present work evaluated synergistic influence of biomolecules with NSs against 4 pathogens. The zone of inhibitions for Chloramphenicol, DMSO and NSs with four concentrations (6.25, 12.5, 25 and 50 µg/µl) are as shown in Fig. 8.

SyG-CuO NSs were found to show better antimicrobial activity against gram positive bacteria than gram negative bacteria which is believed to be due to the structural differences in the cell walls of bacteria. The antimicrobial activity of NSs can be partially attributed to the presence

(cc) BY

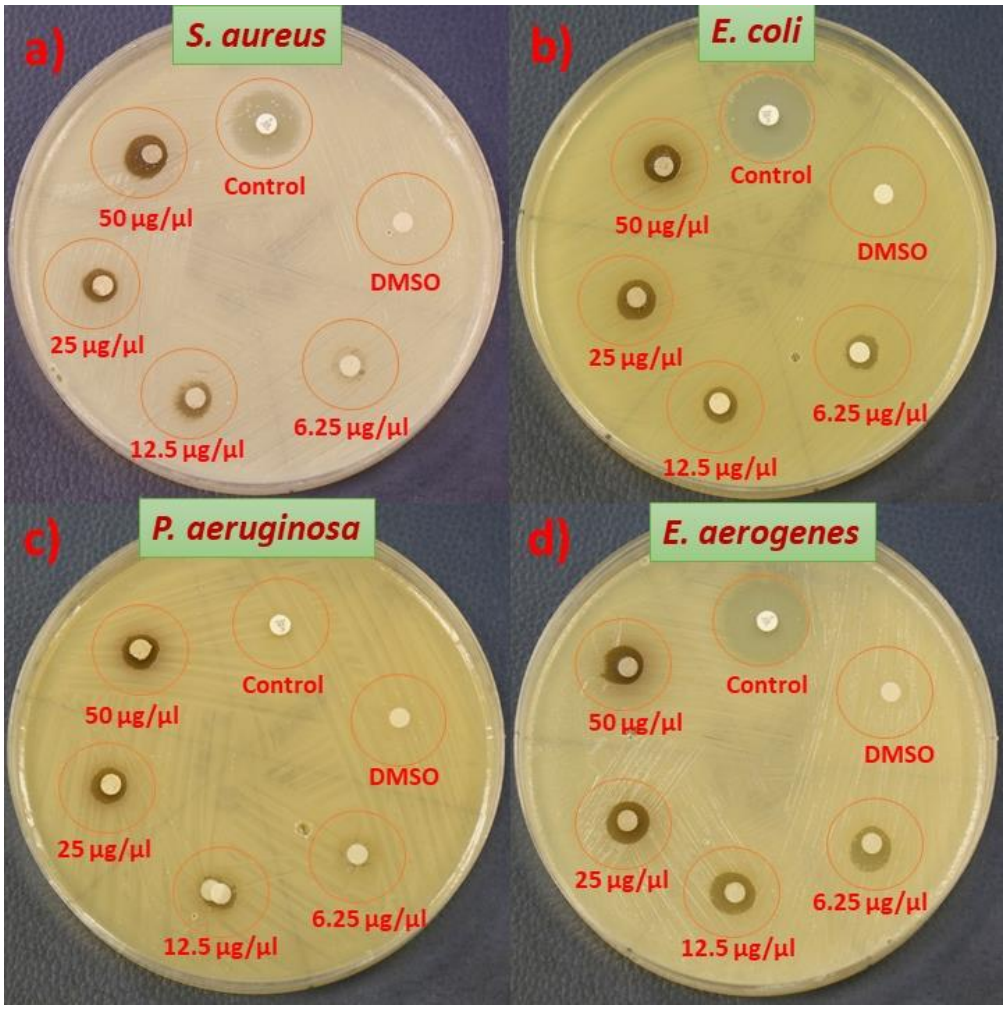

Fig. 8. The antibacterial activity of *SyG*-CuO NSs towards pathogens (a) *S. aureus* (b) *E. coli* (c) *P. aeruginosa* (d) *E. aerogenes.*

of bioactive compounds on the surface of NSs as capping and stabilizing agents. In this regard, the activity was pronounceable against *S. aureus*. The highest zone of inhibition (mm) recorded with 50 µg/µl of *SyG*-CuO NSs against *S. aureus, E. coli and E. aerogenes* bacteria was 12 mm and the lowest zone of inhibition (mm) recorded against P. *aeruginosa* bacteria was 10 mm (Table 3).

Pure Cu and its oxides were proved to exhibit excellent antimicrobial activity. The wide zone of inhibitions (Fig. 8) of *SyG*-CuO NSs against pathogens confirm their superior potentiality to inhibit and cause death of pathogens. It was found that the bacterial resistance decreased with increase in the concentration of the nanoparticles for all the bacteria except *E. aerogenes*. The antimicrobial results obtained using SyG-CuO NSs, were found to be better when compared with earlier results presented by many researchers (Table 4).

The highest zone of inhibition (mm) recorded with CuO NSs against bacteria was 12 mm which is comparatively better than those of zone of CuO NSs synthesised by various researchers using various plant extracts as mentioned in the Table 4. Thus it can be concluded that the cumulative effect of CuO NSs coupled with bioactive compounds such as tannins, saponins and glycosides of *Syzygium guineense* leaf extract proved to be detrimental for bacteria [25].

Even though many antimicrobial mechanisms were proposed by earlier researchers, the action of

CC BY

Table 3. The variation of zone of inhibitions for different bacterial pathogens by *SyG*-CuO NSs.

Concentration of NSs (μg/μl)	Bacterial strains and Zone of Inhibition in mm			
	S. aureus ATCC25923	*E. coli* ATCC25992	*P. aeruginosa* ATCC27853	*E. Aerogenes* ATCC13048
50	12	12	10	12
25	10	12	10	12
12.5	10	10	10	12
6.25	10	10	6	12
Chloramphenicol	20	22	6	28
DMSO	6	6	6	6

Table 4. Comparative statistics of antimicrobial and antifungal activities of $Cu/Cu_2O/CuO$ synthesised by using various plant and algal extracts.

Sl. No.	Plant extract	NSs	Zone of Inhibition (mm)	Tested Pathogens	Reference
1	*Syzygium aromaticum bud*	Cu	7	*E. coli*	[22]
2	*Brassica oleracea var. italic*	CuO	9	*C.albicans*	[23]
3	*Leucaena leucocephala L.*	CuO	11	*P. aeruginosa*	[24]
4	*S. lavandulifolia flower*	Cu/Cu_2O	12	*P. aeruginosa*	[25]
5	*Syzygium guineense leaves*	Cu	12	*E. coli* *S. aureus* *E. aerogenes*	Present work
6	Green and black tea leaves	Cu	14	*S. aureus*	[26]
7	Black grape leaves	Cu	14	*E.coli*	[27]
8	*Hagenia abyssinica (Brace) JF. Gmel.* leaves	$Cu/Cu_2O/CuO$	14.7	*S. aureus*	[7]

SyG-CuO NSs on the bacteria is yet to be explored fully. Nanoparticles were found to cause the death of bacteria by attacking its cell wall, inhibiting RNA synthesis and preventing DNA replication. It is assumed that the positive copper oxide in the NSs get adsorbed on to the cell wall of bacteria and interacts with the negatively charged species. This results in disruption of the cell wall and damage occurred by entering into the cell through the generation of reactive oxygen species (ROS) by the effect of visible/UV light radiation. It is also believed that the synergistic effect of *SyG*-CuO NSs with bioactive compounds of extract would have played significant influence to inhibit the activity of pathogenic bacteria as suggested by the recent researcher.

Most studies have shown that Gram-negative bacterial growth is more affected by NSs than Gram-positive bacteria which can be attributed to thin cell walls that are easily penetrated, while Gram-positive bacteria have thicker cell wall [26]. In addition, electrochemical potential across the cell membrane decreases up on interaction with the released Cu metal ion by *SyG*-CuO NSs affecting integrity of the membrane [27]. The maximum antibacterial activity is recorded with Gram-negative bacteria than the Gram-positive bacteria due to their differences in their cell structure [28].

Electrochemical activity

In order to evaluate the electrode stability of the prepared oxides, a series of CV scans (of 25 cycles), at a scanning rate of 50 mVs^{-1}, for SyG-CuO NSs sample was carried out (Fig. 9). During the test, the locations of anodic and cathodic peaks of electrode did not show any significant deviation with the growing cycles, which confirms good electrode stability [29] [30].

The charge transfer resistance R_{ct} is a direct measure of the diameter of the semicircle arc on the real axis. It can be observed that the impedance curve of SyG-CuO NSs is inclined towards Y axis; this suggests a low capacitance and minimum charge-transfer resistance of prepared electrode [31].

The resistance of the nanomaterial can be obtained using the Nyquist plot. The semicircular portion at a higher frequency is equal to the electron transfer resistance (R_{ct}) at the contact interface of the electrode and electrolyte solution

(cc) BY

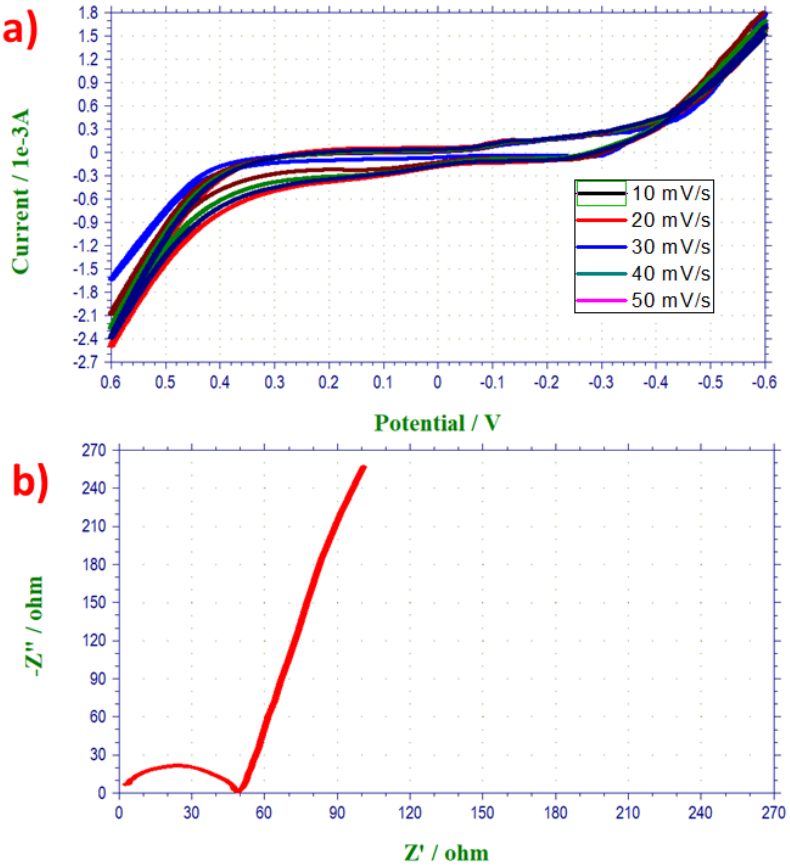

Fig. 9. Cyclic voltammogram and EIS spectra of SyG-CuO NSs at different scan rates.

[32]. As seen in Fig. 9, the semicircular diameter of SyG-CuO NSs is small. The value of R_{ct} is equal to the diameter of the semicircle. The R_{ct} value of SyG-CuO NSs is found to be 49 Ω which confirms that the nanomaterial has considerably good conductivity and thus can be better alternative as electrode material.

CONCLUSION

The application of medicinal plant, *Syzygium guineense* leaf extract towards the green synthesis of copper and its oxides (SyG-CuO) nanostructures was successful. The UV-visible spectra, XRD pattern and FTIR spectra confirmed the formation crystalline SyG-CuO NSs in the presence of biomolecules such as phenolics, tannins, glycosides and proteins of the plant extract. Thermal stability of CuO NSs was confirmed by TGA-DTA analysis. TEM-HRTEM-SAED analysis confirmed the presence of Cu and its oxides. The synergistic influence of bioactive compounds and SyG-CuO NSs proved to be highly effective antibacterial agent against pathogens, Gram positive bacteria *S. aureus,* and Gram negative bacteria, *E. coli, P. aeruginosa,* and *E. aerogenes.* The EIS and CV studies confirmed better electrochemical behavior of SyG-CuO NSs with superior electrode property. The green copper oxide NSs exhibited better future perspective for antimicrobial and electrochemical applications.

ACKNOWLEDGEMENT

The authors are grateful and thankful to Adama Science and Technology University for financial support and laboratory facility to conduct this research work which was funded from the project (ANSD/04/0453/11-2018) approved by Research and Technology Transfer Office, sanctioned by Adama Science and Technology University, Ethiopia.

CONFLICT OF INTEREST

The authors declare that there is no conflict of interests regarding the publication of this manuscript.

REFERENCES

1. Judženti enė A. Wormwood (Artemisia absinthium L.) Oils. Essential Oils in Food Preservation, Flavor and Safety: Elsevier; 2016. p. 849-56.
[2] B. A. and K. S. H. C. Ananda Murthy1, C. H. Prakash, *Current Research in Science and Technology Vol. 4*, vol. 4. Book Publisher International (a part of SCIENCEDOMAIN International), 2020.
[3] G. Sougata and C. Maliyackal, Jini, Chacko,. Ashwini, N, Harke,. Sonal, P, Gurav,. Komal, A, Joshi,. Aarti, Dhepe,. Anuja, S, Kulkarni,. Vaishali, S, Shinde,. Vijay, Singh, Parihar,. Adersh, Asok,. Kaushik, Banerjee,. Narayan, Kamble,. Jayesh, Bellare,. Balu, A, "Nanomedicine & Nanotechnology Barleria prionitis Leaf Mediated Synthesis of Silver and Gold," *Journal of Nanomedicine & Nanotechnology*, vol. 7, no. 4, 2016.
4. Ghosh S, Jagtap S, More P, Shete UJ, Maheshwari NO, Rao SJ, et al. Dioscorea bulbiferaMediated Synthesis of Novel AucoreAgshellNanoparticles with Potent Antibiofilm and Antileishmanial Activity. Journal of Nanomaterials. 2015;2015:1-12.
[5] and D. P. N. Saranya Sukumar, Agneeswaran Rudrasenan, "Green synthesis of Cu/Cu_2O/CuO nanostructures and the analysis of their electrochemical properties," *ACS omega*, vol. 5, no. 2, p. 1040, May 2020.
6. Murthy HCA, Desalegn Zeleke T, Ravikumar CR, Anil Kumar MR, Nagaswarupa HP. Electrochemical properties of biogenic silver nanoparticles synthesized using Hagenia abyssinica (Brace) JF. Gmel. medicinal plant leaf extract. Materials Research Express. 2020;7(5):055016.
7. Shume WM, Murthy HCA, Zereffa EA. A Review on Synthesis and Characterization of Ag2O Nanoparticles for Photocatalytic Applications. Journal of Chemistry. 2020;2020:1-15.
8. Murthy HCA, Desalegn T, Kassa M, Abebe B, Assefa T. Synthesis of Green Copper Nanoparticles Using Medicinal Plant Hagenia abyssinica (Brace) JF. Gmel. Leaf Extract: Antimicrobial Properties. Journal of Nanomaterials. 2020;2020:1-12.
9. Kumar MRA, Ravikumar CR, Nagaswarupa HP, Purshotam B, Gonfa B, Murthy HCA, et al. Evaluation of bi-functional applications of ZnO nanoparticles prepared by green and chemical methods. Journal of Environmental Chemical Engineering. 2019;7(6):103468.
10. Ananda Murthy HC, Abebe B, C H P, Shantaveerayya K. A Review on Green Synthesis and Applications of Cu and CuO Nanoparticles. Material Science Research India. 2018;15(3):279-95.
[11] A. Bagheri, H. Halakouie, D. Ghanbari, M. Mousayi, and N. Asiabani, "Strontium Hexa-ferrites and polyaniline nanocomposite: Studies of magnetization, coercivity, morphology and microwave absorption," *Journal of Nanostructures*, vol. 9, no. 4, pp. 630–638, 2019.
[12] Z. Sorinezami and D. Ghanbari, "Facile preparation of silver nanoparticles and antibacterial Chitosan-Ag polymeric nanocomposites," *Journal of Nanostructures*, vol. 9, no. 3, pp. 396–401, 2019.
13. Abebe B, Murthy HCA, Amare E. Enhancing the photocatalytic efficiency of ZnO: Defects, heterojunction, and optimization. Environmental Nanotechnology, Monitoring & Management. 2020;14:100336.
14. Roy A, Bulut O, Some S, Mandal AK, Yilmaz MD. Green synthesis of silver nanoparticles: biomolecule-nanoparticle organizations targeting antimicrobial activity. RSC Advances. 2019;9(5):2673-702.
15. Azarbani F, Shiravand S. Green synthesis of silver nanoparticles by Ferulago macrocarpa flowers extract and their antibacterial, antifungal and toxic effects. Green Chemistry Letters and Reviews. 2020;13(1):41-9.
16. Yaqub A, Malkani N, Shabbir A, Ditta SA, Tanvir F, Ali S, et al. Novel Biosynthesis of Copper Nanoparticles Using Zingiber and Allium sp. with Synergic Effect of Doxycycline for Anticancer and Bactericidal Activity. Current Microbiology. 2020;77(9):2287-99.
17. Sreeju N, Rufus A, Philip D. Nanostructured copper (II) oxide and its novel reduction to stable copper nanoparticles. Journal of Physics and Chemistry of Solids. 2019;124:250-60.
18. Bhosale MA, Bhanage BM. A facile one-step approach for the synthesis of uniform spherical Cu/Cu_2O nano- and microparticles with high catalytic activity in the Buchwald–Hartwig amination reaction. RSC Adv. 2014;4(29):15122-30.
19. Avinash B, Ravikumar CR, Kumar MRA, Nagaswarupa HP, Santosh MS, Bhatt AS, et al. Nano CuO: Electrochemical sensor for the determination of paracetamol and d-glucose. Journal of Physics and Chemistry of Solids. 2019;134:193-200.
20. Sánchez-Sanhueza G, Fuentes-Rodríguez D, Bello-Toledo H. Copper Nanoparticles as Potential Antimicrobial Agent in Disinfecting Root Canals: A Systematic Review. International journal of odontostomatology. 2016;10(3):547-54.
21. Eskandari N, Nabiyouni G, Masoumi S, Ghanbari D. Preparation of a new magnetic and photo-catalyst $CoFe_2O_4$–$SrTiO_3$ perovskite nanocomposite for photo-degradation of toxic dyes under short time visible irradiation. Composites Part B: Engineering. 2019;176:107343.
22. Fuku X, Modibedi M, Mathe M. Green synthesis of Cu/Cu_2O/CuO nanostructures and the analysis of their electrochemical properties. SN Applied Sciences. 2020;2(5).
23. Nadagouda MN, Iyanna N, Lalley J, Han C, Dionysiou DD, Varma RS. Synthesis of Silver and Gold Nanoparticles Using Antioxidants from Blackberry, Blueberry, Pomegranate, and Turmeric Extracts. ACS Sustainable Chemistry & Engineering. 2014;2(7):1717-23.
24. Cheirmadurai K, Biswas S, Murali R, Thanikaivelan P. Green synthesis of copper nanoparticles and conducting nanobiocomposites using plant and animal sources. RSC Advances. 2014;4(37):19507.
25. Chen J, Mao S, Xu Z, Ding W. Various antibacterial mechanisms of biosynthesized copper oxide nanoparticles against soilborneRalstonia solanacearum. RSC Advances. 2019;9(7):3788-99.

CC BY

26. Anbu P, Gopinath SCB, Yun HS, Lee C-G. Temperature-dependent green biosynthesis and characterization of silver nanoparticles using balloon flower plants and their antibacterial potential. Journal of Molecular Structure. 2019;1177:302-9.
27. Thangamani N, Bhuvaneshwari N. Green synthesis of gold nanoparticles using Simarouba glauca leaf extract and their biological activity of micro-organism. Chemical Physics Letters. 2019;732:136587.
28. Muthuvel A, Jothibas M, Manoharan C. Synthesis of copper oxide nanoparticles by chemical and biogenic methods: photocatalytic degradation and in vitro antioxidant activity. Nanotechnology for Environmental Engineering. 2020;5(2).
29. Kumar MRA, Abebe B, Nagaswarupa HP, Murthy HCA, Ravikumar CR, Sabir FK. Enhanced photocatalytic and electrochemical performance of TiO_2-Fe_2O_3 nanocomposite: Its applications in dye decolorization and as supercapacitors. Scientific Reports. 2020;10(1).
30. Abebe B, Murthy HCA, Zerefa E, Adimasu Y. PVA assisted ZnO based mesoporous ternary metal oxides nanomaterials: synthesis, optimization, and evaluation of antibacterial activity. Materials Research Express. 2020;7(4):045011.
31. T. R. S. S, H. C. A. M. V.V. Deshmukh, H.P. Nagaswarupa, C.R. Ravikumar, M.R. Anil Kumar, "Asian Journal of Chemsitry," *Asian Journal of Chemistry*, vol. 32, no. 8, pp. 2013–2020, 2020.
32. Mir JF, Rubab S, Shah MA. Photo-electrochemical ability of iron oxide nanoflowers fabricated via electrochemical anodization. Chemical Physics Letters. 2020;741:137088.

CC BY